

# Wildfire Potential Mapping over the State of Mississippi: A Land Surface Modeling Approach

**William H. Cooke<sup>1</sup>**

*Department of Geosciences and Geosystems Research Institute,  
Mississippi State University Mississippi State, Mississippi 39762*

**Georgy V. Mostovoy**

*Geosystems Research Institute, Mississippi State University,  
Mississippi State, Mississippi 39762*

**Valentine G. Anantharaj**

*National Center for Computational Sciences,  
Oak Ridge National Laboratory, Oak Ridge, Tennessee 37831*

**W. Matt Jolly**

*U.S. Forest Service, Rocky Mountain Research Station,  
Fire Sciences Laboratory, Missoula, Montana 59808*

---

**Abstract:** A relationship between the likelihood of wildfires and various drought metrics (soil moisture-based fire potential indices) were examined over the southern part of Mississippi. The following three indices were tested and used to simulate spatial and temporal wildfire probability changes: (1) the accumulated difference between daily precipitation and potential evapotranspiration ( $P - E$ ); (2) simulated moisture content of the top 10 cm of soil; and (3) the Keetch-Byram Drought Index (*KBDI*). These indices were estimated from gridded meteorological data and Mosaic-simulated soil moisture data available from the North American Land Data Assimilation System (NLDAS-2). The relationships between normalized fire potential index deviations and the probability of at least one fire occurring during the following five consecutive days were evaluated using a 23-year (1986–2008) forest fire record for an evenly spaced grid ( $0.25^\circ \times 0.25^\circ$ ) across the state of Mississippi's coastal plain. Two periods were selected and examined (January–mid June and mid September–December). There was good agreement between the observed and logistic model-fitted fire probabilities over the study area during both seasons. The fire potential indices based on the top 10 cm soil moisture and *KBDI* had the largest impact on wildfire odds, increasing it by almost 2 times in response to each unit change of the corresponding fire potential index during January–mid-June period and by nearly 1.5 times during mid-September–December. These results suggest that soil moisture-based fire potential indices are good indicators of fire occurrence probability across this region.

---

---

<sup>1</sup>Corresponding author; email: whc5@geosci.msstate.edu

## INTRODUCTION

Occurrence, intensity, and potential spread of wildfires over a given area depends on many factors such as soil moisture content, vegetation type and structure, fuel availability, fire history, weather, topography, and human factors (e.g., proximity to city limits, roads, recreation areas, etc.). Due to the hazardous nature of wildfire, regional assessments and regular mapping of fire probability based on these factors is an important practical task (Chou et al., 1993, p. 129). A number of these factors or even one particular factor can be converted into a fire potential index that quantifies wildfire likelihood over a given region, (e.g., Choi et al., 2009; Chéret and Denux, 2011). Because forest wildfires occur more frequently during severe droughts associated with negative anomalies of atmospheric precipitation, the soil moisture content is a good fire potential indicator. Zhai et al. (2003) have described the effects of various human, economical, geographical, and timber-related factors on forest fire probability.

Water deficits affect many components of the wildland fuel complex such as organic soils, fine and coarse dead fuels, and live vegetation. As water deficits increase, fuels become drier, making them ignite and burn more readily (Dimitrakopoulos et al., 2010, p. 31). Smoldering potential in organic soils is strongly influenced by its moisture content (Reardon, 2007, p. 113). Pook and Gill (1993) have demonstrated that soil moisture deficit metrics are closely related to surface litter dead fuel moisture. Albin and Reinhardt (1995) have shown that moisture also regulates the ignition delay timing and the burning rate of large-diameter, dead fuels such as logs and branches. Pellizzaro and coauthors (2007) have recognized that seasonal changes in live fuel moisture are closely related to changes in water availability and are best predicted using simple drought metrics. Additionally, Chladil and Nunez (1995) have concluded that seasonal senescence, or curing, of herbaceous vegetation is regulated by soil moisture deficits. Given that water availability strongly influences most wildland fuel components in some way, soil moisture deficit metrics have the potential to serve as proxies for wildland fire potential.

Various drought indicators and indices having a different level of complexity are developed to describe different aspects of drought conditions (short- and long-term, atmospheric, agricultural/ecological, and hydrological) associated with impacts on soil moisture, vegetation, and surface waters (e.g., Heim, 2002, p. 1151; Swain et al., 2011). In this study, three soil moisture-based indices are used to map and characterize the fire potential over the Mississippi coastal plain. These three moisture indices range from (1) a simple accumulated difference between daily precipitation ( $P$ ) and potential evapotranspiration ( $E$ ) (hereafter referred to as  $P-E$ ) to the (2) Keetch-Byram drought index ( $KBDI$ ), which accounts parametrically for vegetation density effects on evapotranspiration in forested areas, and (3) the top 10 cm soil moisture (SM) content, simulated with a state-of-the-art land surface model (LSM), which provides the most complete physical description of water movement within an isolated soil column and accounts for corresponding changes of water/energy balance on the vegetation-covered soil surface. Major features of these drought indices are presented in Table 1. Note that all the indices are associated with the soil moisture content but  $KBDI$  mimics the moisture deficit within the top soil layer.

Generally, the fire risk indices such as  $P-E$  or  $KBDI$  are calculated using conventional *in situ* meteorological data (e.g., precipitation and daily maximum air

**Table 1.** Drought Indices Used in This Paper

Index	Modeling approach	Application	Soil column depth	Soil water availability	Evaporation rate	Vegetation
Based on accumulated P-E (Choi et al., 2009)	Simplified "bucket-type" soil water balance model (Manabe and Delworth, 1990)	Upper soil layer	Not defined	Infinitive	Potential (E)	None
Keetch-Byram Drought Index (Keetch and Byram, 1968)	Based on deficit estimates of soil moisture from a single-layer water balance model	Duff and upper soil layer	Not defined, depends on actual soil type	20.32 cm (8 inches, constant)	Function of maximum daily temperature and mean annual precipitation	Vegetation density is parameterized in terms of mean annual precipitation
Based on top 0–10 cm moisture content	Simulations with the state-of-the-art Mosaic land surface model (Koster and Suarez, 1992) having three soil layers	0–200 cm	200 cm	Depends on soil type (texture)	Function of E, atmospheric surface and layer resistance, and of weighted soil moisture deficit within 0–200 cm	Vegetation type/class is specified and vegetation fraction reflects most recent multi-year mean conditions

temperature) available from the state observational network (NOAA NCDC, 2009). Because these routine observations are typically separated by a distance of 30–50 km or more in the case of *in situ* observations of potential evapotranspiration (Cooke et al., 2008, p. 153), a spatial interpolation is necessary to estimate fire indexes at a regular grid with a spacing less than 10 km (Janis et al., 2002, p. 284). An alternative approach adopted in the present study involves use of gridded meteorological data instead of the surface station data for the fire potential assessments. Recently, the high-quality hourly surface meteorological data gridded over the continental United States region (and some adjacent areas of Canada and Mexico) at 0.125° latitude/longitude spacing has become available to the research community as a part of the North American Land Data Assimilation System (NLDAS), described by Mitchell et al. (2004). This system provides the necessary sensible surface weather parameters needed to calculate the aforementioned fire potential metrics. Data from the latest version of NLDAS (Phase 2 or NLDAS-2) are available for a 31-year period (1980–2010).

The objective of the study was to demonstrate applicability of NLDAS meteorological data and Mosaic Land Surface Model (LSM) simulated soil moisture for mapping/assessing the fire risk across the Mississippi coastal plain. Considering that this comprehensive source (NLDAS and LSM-simulated fields) of meteorological and environmental data are rather new, a regional test of these data within a fire risk assessment system looks natural. *P-E*, *KBDI*, and soil moisture indices were derived from NLDAS surface meteorology and were compared to a 23-year record (1986–2008) of fire occurrence. The resulting probabilistic models were evaluated to determine the strength of the relationships between these drought metrics and the likelihood of fires across this region.

## METHODS

### *Land Surface Modeling Data*

The following atmospheric variables from the NLDAS-2 project were used in this study: precipitation, potential evapotranspiration, and the air temperature. All these variables available at hourly basis were aggregated to daily accumulated values (*P* and *E*) except for the air temperature, which was converted to the daily maximum temperature ( $T_{max}$ ) by selecting the maximum among the hourly values.

The overall quality of NLDAS variables was validated against point observations and has proven high. For example, Luo and coauthors (2003) performed an evaluation study over the Southern Great Plains, spanning almost a two-year period and showing that typical standard deviations between NLDAS variables and those observed at surface stations are 2.3°C (for the air temperature), 1.1 g/kg (for the water vapor specific humidity), 1.5 m/s (for the wind speed), and 0.65 mm/hr and 0.15 mm/hr (for the hourly and daily precipitation rates, respectively).

The hourly precipitation data in NLDAS-2 are based on daily precipitation reanalysis, produced from gauge reports at the NCEP Climate Prediction Center. The observed daily precipitation rates were disaggregated into the hourly values using weights derived from the Next-Generation radar (NEXRAD) observations at 4 × 4 km<sup>2</sup> resolution. The downward solar radiation flux at the surface is retrieved from NOAA's GOES satellite measurements. The other NLDAS-2 atmospheric fields are

spatially and temporally interpolated from the North American Regional Reanalysis (NARR) fields produced at 32 km grid spacing every 3 hours as described by Mesinger et al. (2004). The interpolation procedures are summarized by Cosgrove et al. (2003).

In addition to these atmospheric surface data, the soil moisture simulated with the Mosaic Land Surface Model (LSM) developed by Koster and Suarez (1992) are also available at the NLDAS web archive in a near-real-time mode. The normalized fire risk indexes were derived from the NLDAS-2 atmospheric data ( $P$ ,  $E$ , and  $T_{max}$  variables) and the top 10 cm soil moisture content (Mosaic-simulated).

The Mosaic LSM explicitly accounts for sub-grid vegetation heterogeneity using the tile approach (the model allows up to 10 tiles having different vegetation type within the grid cell). The NLDAS-2 configuration of Mosaic model has three soil layers with the following thickness: 10, 30, and 160 cm. The soil moisture content in each layer is predicted from a numerical solution of a diffusion equation. The solution depends on soil hydraulic properties such as saturated conductivity, matrix potential, porosity, and others. The force-restore method is adopted in the Mosaic model to predict the soil temperature in two layers (surface and deep) only (Koster and Suarez, 1992, p. 2699). Note that the surface temperature ( $T_s$ ), which is equal to canopy temperature, is estimated from the prognostic energy balance equation. Therefore, the Mosaic LSM implies some heat storage (the term  $\partial T_s / \partial t$  is nonzero) within the thin surface layer having a finite thickness, which includes both the soil substrate and the canopy air. Surface static fields (vegetation fraction, leaf and stem area indices, soil porosity and texture, sand/clay/silt fraction, slope, and others), which are a necessary input to the Mosaic LSM, are bilinearly interpolated or aggregated from their native grids (most of these fields are available at  $0.01^\circ$  grid spacing) to the NLDAS-2 Mosaic  $0.125^\circ \times 0.125^\circ$  latitude-longitude grid. In order to estimate the soil moisture and other surface states, the Mosaic LSM is integrated numerically using the NLDAS-2 atmospheric forcing fields. Finally, the Land Information System (LIS) software allows simulations of surface and subsurface states (including soil moisture) with Mosaic LSM (a set of different LSMs are also available) at any geographical region and at the spatial grid spacing starting from 1 km, as described by Kumar et al. (2008).

### *Fire Data*

Wildfire records (dates, geographical coordinates, and total area burnt) for 18 years (1991–2008) for the state of Mississippi were obtained from the Mississippi Forestry Commission inventory (Grala and Cooke, 2010, p. 16). Another 5 years (1986–1990) of wildfires data were downloaded from <http://www.fs.fed.us/fire/fuelman/fireloc.htm> (Preisler et al., 2004, p. 134). These data sets were combined into a 23-year-long database that describes timing, location, and size of fires that occurred on both federal and state lands. Only relatively large fires having a burning area more or equal to 16 acres (6.48 ha) were used.

### *Fire Potential Indices*

All fire potential indices used in the study represent a certain surrogate (or approximation) of the soil water content described by a water budget equation. The water budget equation for the soil column of an arbitrary depth can be written as follows:

$$\frac{dw}{dt} = P - Ef(w) - Q_s(w) \quad (1)$$

where  $w$  is the soil column water content (soil moisture),  $f(w)$  is the function that relates actual evaporation to the potential evaporation  $E$ , and  $Q_s(w)$  describes the water losses rate via surface runoff and percolation through the bottom of the soil column. Note that both  $f(w)$  and  $Q_s(w)$  are nonlinear functions of  $w$ . The equation (1) can be rewritten for the soil moisture deficit ( $w_s - w$ ) as follows:

$$\frac{d(w_s - w)}{dt} = -(P - Ef(w) - Q_s(w)) \quad (2)$$

where  $w_s$  is the saturated value of the soil moisture.

The integral of Eq. (1) shows that accumulated values of  $(P-E)$  represent the simple measure of the soil moisture content change (relative to some reference value describing an initial state of the soil moisture), provided that  $f(w) = 1$  and  $Q_s(w) = 0$  (evaporation rate is equal to potential and there is no loss of water due to the surface runoff and percolation). The resulting soil moisture content can be considered as that produced by a simplified version of a simple “bucket-type” LSM representing the soil column as a water reservoir (water storage bucket) introduced by Manabe and Delworth (1990) and having an infinite capacity. The upper frame in Figure 1 illustrates an example of accumulated  $(P-E)$  time series beginning January 1 of every year with zero soil water content ( $w = 0$ ) for the grid cell located in the southern part of the state of Mississippi (near 30.6° N and 89.2° W). The thick line depicts the 31-year mean annual cycle of accumulated  $(P-E)$  and a standard deviation from the mean is shown by shading. The mean soil moisture (as estimated by the accumulated  $P-E$  values) increases gradually to the end of February, remains approximately constant for some time, and then begins to deplete monotonically from the end of March to the end of year. Long-term simulations using the Mosaic LSM provides a more realistic annual mean cycle of soil moisture, as illustrated in the middle frame in Figure 1. Finally, the lower frame in Figure 1 shows the mean annual cycle of  $KBDI$ , which essentially is a mirror image of the annual cycle based on the top 10 cm soil moisture. The Keetch-Byram Drought Index ( $KBDI$ ) was calculated as described by Keetch and Byram (1968) and by Janis et al. (2002).

Any given year may be viewed as a realization (or a sample sequence) of a random (stochastic) process and for a fixed day one gets the random variable (Jazwinski, 2007, p. 48). The sample sequences of accumulated  $(P-E)$ , top 10 cm soil moisture, and  $KBDI$  are shown in Figure 1 by red dashed lines for year 2008. The sample sequences for each year were converted into z-scores (Wilks, 2006, p. 47) or standardized anomalies by subtracting the 31-year mean from the original value and dividing the result by the standard deviation. It was assumed that such normalization provides more robust and adequate description of temporal dynamics of soil moisture anomalies than the original (not normalized) indexes and that it ensures that indices are comparable between geographic areas where potential index ranges may vary. The standardized anomalies based on accumulated  $(P-E)$ ,  $KBDI$ , and the top 10 cm soil moisture variables are depicted in Figure 2 for the year 2008. We will call them fire potential indices based on  $(P-E)$ , top 10 cm soil moisture, and  $KBDI$ . For easy comparison and consistency, the  $KBDI$ -based fire risk index shown in Figure 2 was multiplied by  $-1$ . Note that all

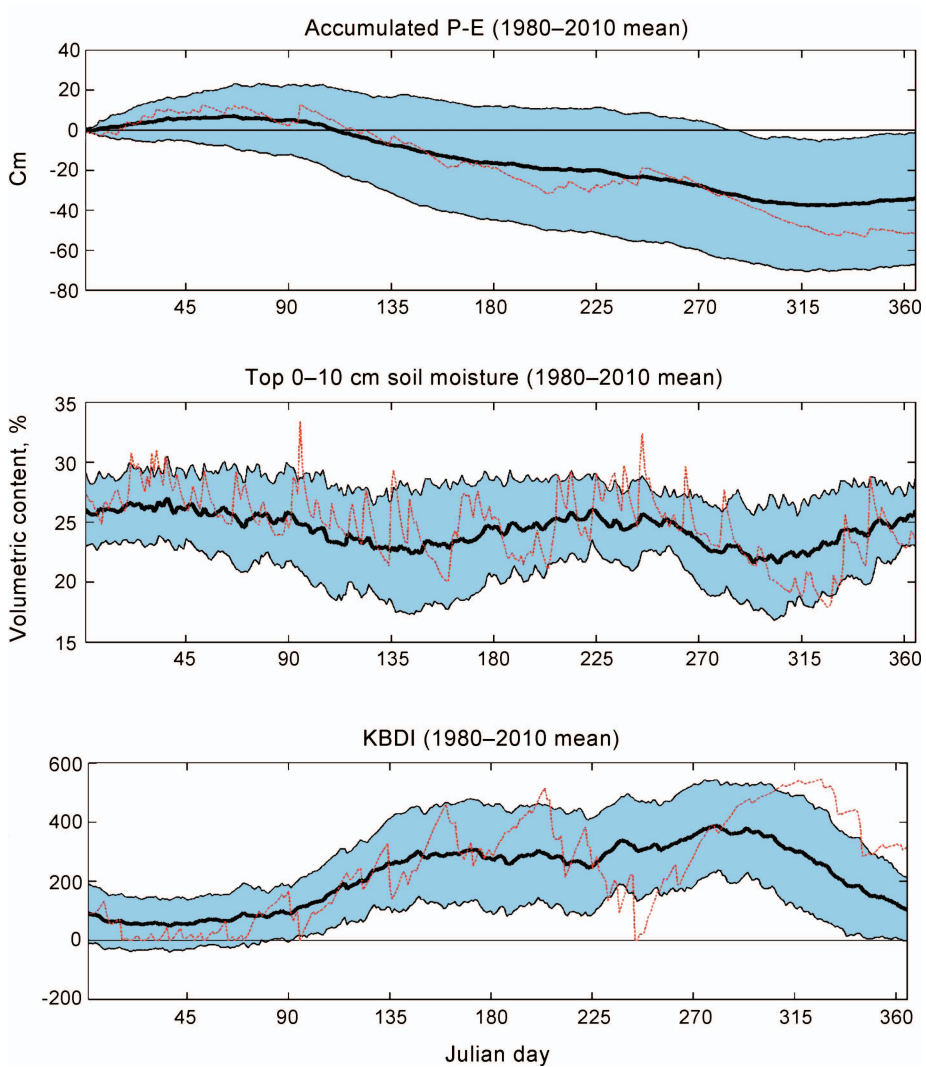


**Fig. 1.** Time series of accumulated  $P-E$  (upper frame), top 10 cm soil moisture (middle), and  $KBDI$  (lower frame) daily values for the grid cell near  $30.6^\circ \text{ N}$  and  $89.2^\circ \text{ W}$ . Thick lines represent the 1980–2010 mean and dashed lines the year 2008. Shading shows standard deviation from the mean.

indexes are related to the soil water content ( $w$ ) but  $KBDI$  describes the soil moisture deficit ( $w_s - w$ ).

Figure 2 provides a comparison among annual cycles of the fire potential for a grid cell located close to the Mississippi Coast during 2008. The major common maximum and minimum of the annual cycle (e.g., maximum in late winter–early spring, the summer minimum, and maximum during the fall, followed by the gradual decrease to the end of December) are quite well reproduced by the different fire potential indexes.

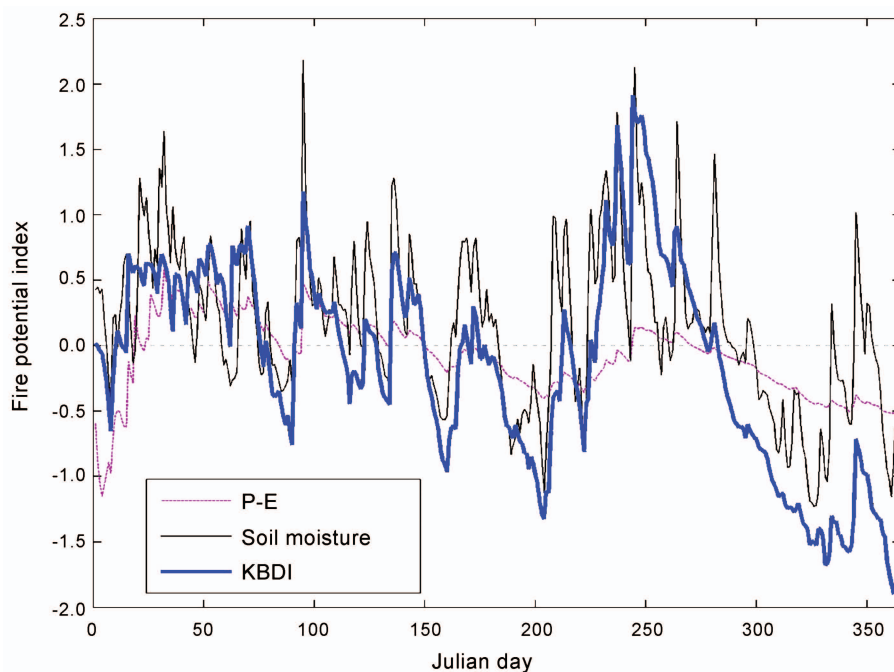


**Fig. 2.** Time series of fire potential indices based on accumulated  $P-E$ , top 10 cm soil moisture, and KBDI for the grid cell near  $30.6^{\circ}$  N and  $89.2^{\circ}$  W during 2008.

Note that the ( $P-E$ )–based index provides a rather smooth annual cycle in comparison to the other two fire risk indices.

In order to better illustrate and understand spatial and interannual variations of the fire potential indices and their relation to fire occurrence at monthly basis, Figure 3 shows the geographical distribution of monthly-mean values over the state of Mississippi during March 2001 (relatively small number of fires), 2002 (high number of fires), 2003 (small number of fires), and 2008 (extremely high number of fires). An overall good agreement is observed between areas of low fire indices shown in blue in Figure 3 and the locations of fire events. On average, the number of fire locations increases in response to lowering values of fire indices and interannual variability of number of fires is related to fire index variations in the same way. Also, there is a general agreement in geographical patterns produced by different indices, although at some areas substantial deviations or biases among them may occur, as illustrated by Figure 3.

#### *Mapping Wildfire Probability*

Probability-based approaches are a natural and effective way to describe the relationship between daily occurrence of fire events within a particular area (it could be a region with a typical size of  $10 \times 10$  km<sup>2</sup> or more) and fire potential index observed over the same area (e.g., Anderson et al., 2000, p. 361; Preisler et al., 2004, p. 136). The knowledge of wildfire event probability and wildfire temporal dynamics (e.g.,



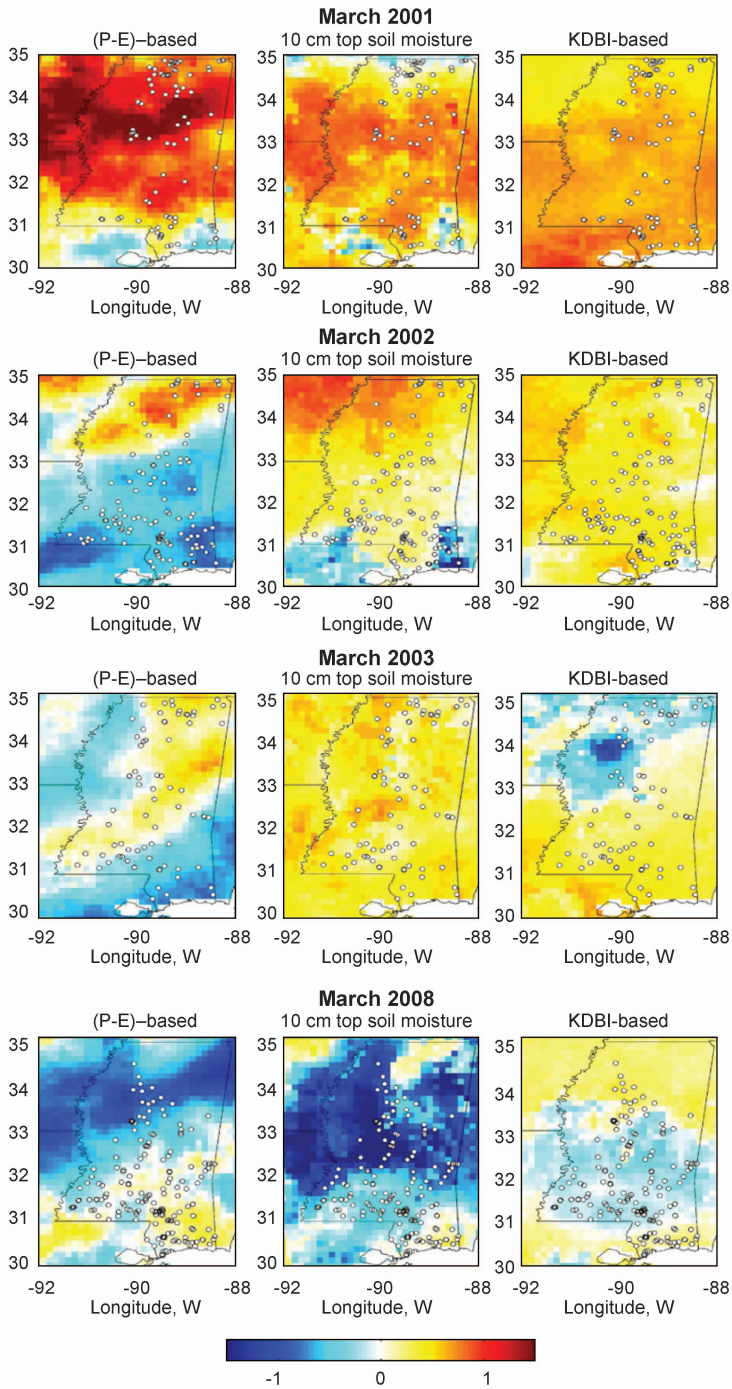


**Fig. 3.** Geographical distribution of fire potential index (mean for March) estimated using *P-E* (left column), the top 10 cm soil moisture (middle), and *KBDI* (right column) data. Small circles represent wildfire locations observed during March.

increasing or lowering of fire odds) over a specific area and during a certain time period (day or week) for a given soil moisture condition (described by the fire potential index) is of paramount importance for forest and natural resources managers. Dividing the fire potential index random variable  $X$  into a finite number of categories (for instance, represented by  $k$  intervals) for this area, fire occurrence probability ( $p_i$ ) can be written as a conditional expectation as follows:

$$p_i = E\left(\frac{Y_i}{N_i} \middle| X_i\right), \quad i = 1, 2, \dots, k \quad (3)$$

where  $X_i$  is the fire risk random variable for the  $i$ -th category,  $N_i$  is the total number of risk indexes within the  $i$ -th category, and  $Y_i$  is the number of observed fires having the risk index within the  $i$ -th category. It is assumed that the natural logarithm of the odds [ $p_i/(1-p_i)$ ] for the fire event is a linear function of  $X_i$ :

$$\log\left(\frac{p_i}{1-p_i}\right) = a_0 + a_1 x_i \quad (4)$$

Equation 4 describes a generalized linear regression model (also known as a logistic regression) for a single explanatory variable  $X_i$  (e.g. McCullagh and Nelder, 1991, p. 110). Note that many other independent explanatory variables can be added within the logistic regression model (e.g., Chou et al., 1993, p. 134). These may include state of weather, wind speed, air relative humidity and temperature, *KBDI*, and other variables (Preisler et al., 2004, p. 136). Due to the multiplicative character of the logistic model (4), any additional variable/covariate ( $Z$ , for example) will result in the extra exponential factor ( $\exp[-\alpha_2 z_i]$ ) in the denominator of Eq. (5).

Equation 4 can be rewritten in the explicit form for the fire probability  $p_i$  as follows:

$$p_i = 1 / (1 + \exp[-a_0 - a_1 x_i]) \quad (5)$$

The maximum likelihood approach (routine *glmfit* available from the MatLab software) was used to estimate the unknown parameters  $\alpha_0$  and  $\alpha_1$  of the logistic regression model. It follows from Equation 4 that the factor  $\exp(\alpha_1)$  describes the multiplicative effect of a unit change in  $X$  on the odds of the fire event. If, for example,  $\exp(\alpha_1) > 1$  (when  $\alpha_1 > 0$ ), the odds of the fire will increased by the factor  $\exp(\alpha_1)$  in response to a unit change in  $X$ . Contrary, if  $\exp(\alpha_1) < 1$  (when  $\alpha_1 < 0$ ), the odds of the fire will lowered by the factor  $\exp(\alpha_1)$ . A zero value of  $\alpha_1$  means that the odds will not be changed ( $\exp[\alpha_1]= 1$ ). Given this simple relationship between the factor  $\exp(\alpha_1)$  and corresponding changes in the fire odds, we will map this factor over the southern part of the state of Mississippi (south of 32° N) to illustrate the controlling impact of different soil moisture indexes on fire probability. The logistic regression model will be applied over the southern part of the state of Mississippi for 0.25° × 0.25° latitude/longitude grid cells (elementary sampling areas) to represent probability of at least one fire occurrence within the cell during five consecutive days. Note that the higher the factor  $\exp(\alpha_1)$ , the greater is controlling effect of the soil moisture on expected fire probability.

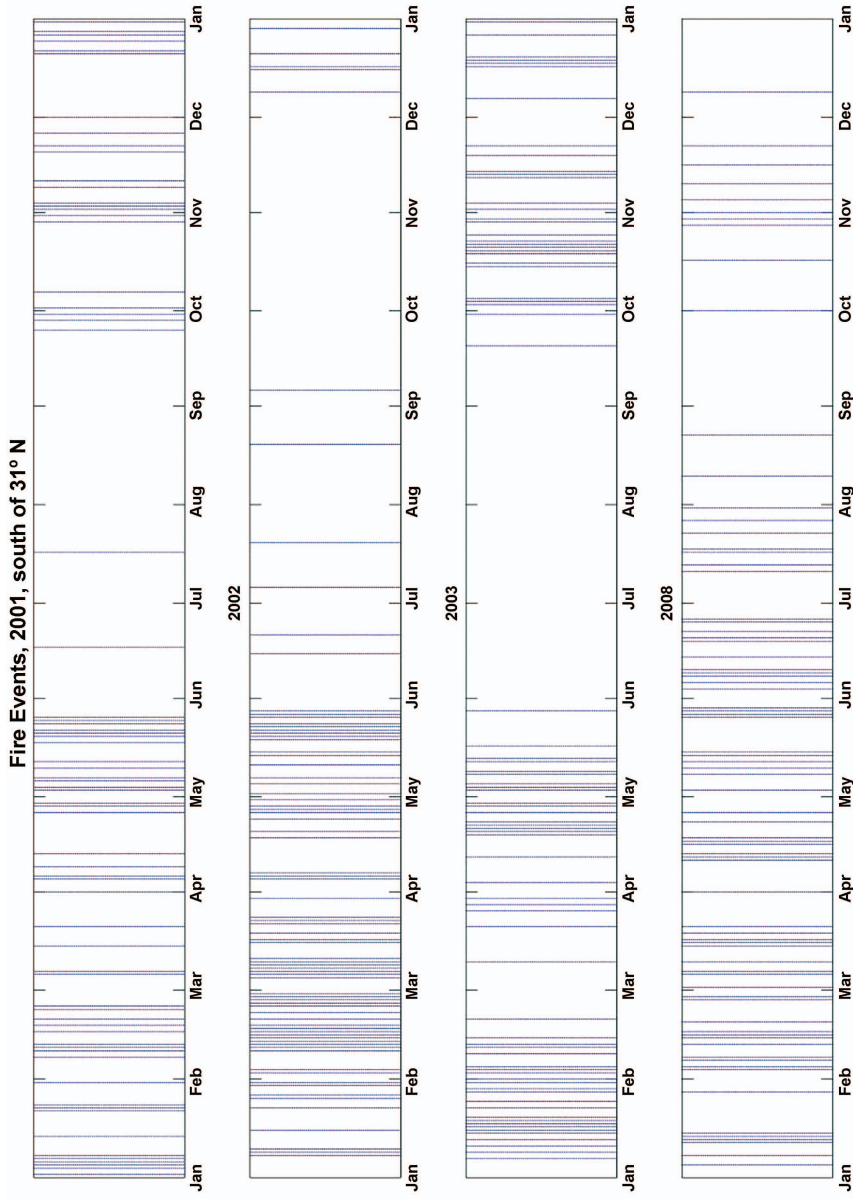


Fig. 4. Fire events distribution south of 31° N for 2001, 2002, 2003, and 2008.

Note that prediction of fire occurrence probability represents a rather simple task in comparison to probability prediction of the fire size (area burnt) and, particularly large fires. Generally, two metrics have been used to account for probability of large fires within the logistic regression framework. One reflects long-term drought conditions related to the moisture deficit (e.g., it could be *KBDI*-based drought index) and another metric—the current weather impact (high surface winds and air temperature and low air humidity), as described by Bradstock et al. (2009). Further, fire risk analysis requires even more elaborative approaches involving assessment of burn probabilities, as suggested by Finney (2005).

## RESULTS AND DISCUSSION

The logistic regression model in Equation 4 can be applied to assess unknown probabilities  $p_i$  of a fire event (occurrence of at least one fire) observed over an arbitrary sampling area during an arbitrary time interval (day or week, for example). For a given number of  $X_i$  discrete intervals, the area should be large enough to provide sufficient number of fire events within each interval  $i$ , in order to get statistically stable/robust estimates of the regression model parameters in Equation 4. The same restriction of having enough fire events is applied for the selection of the time interval. Use of rather small area and time interval can result in unstable estimates (the iteration procedure used by the *glmfit* might result in loss of convergence). The choice of the elementary sampling area and the interval depends on the length of the available record of wildfires. As with any statistically based approach, the logistic model implies a certain degree of the vegetation and landscape homogeneity within each elementary sampling unit and during the sampling period. So, the sampling area and interval cannot be too large because it may violate the assumption of sampling homogeneity. On the other hand, the sampling area cannot be too small as well. If the sampling unit is too small, a single fire event can burn most of the sampling area, thus suppressing future fire events and thus violating statistical independence of fire occurrences. Because we focused on the southern geographical area of Mississippi that is dominated by pine forests (the famous pine belt) and the most common wildfires in Mississippi are incendiary/arson fires, which represent about 60% of all fires (e.g., Grala and Cooke, 2010, p. 22), the assumption of sampling homogeneity can be approximately accepted. Within the logistic regression approach, the user always has a certain degree of freedom to manipulate the sampling area and interval size in order to relax or tighten the above constraints of sampling homogeneity and independence of fire events.

The model parameters ( $\alpha_0$  and  $\alpha_1$ ) were evaluated separately during January–middle of June and during middle of September–December using wildfire data record and soil moisture fire indexes for 23 years (1986–2008). A rather coarse space ( $0.25^\circ \times 0.25^\circ$ ) and time (five-day) resolution were selected in order to meet sampling requirements for the logistic model, mentioned in the previous paragraph. For the same reason, the logistic model was applied over rather broad periods (5.5 and 3.5 months). This choice is partly justified by the annual cycle of wildfire frequency in Mississippi, having a major maximum in March and secondary maximum in October (Grala and Cooke, 2010, p. 20). Additional support for selection of January–mid-June and mid-September–December sampling periods is illustrated by Figure 4. Indeed, the fires are very rare during the summer in comparison to other seasons.

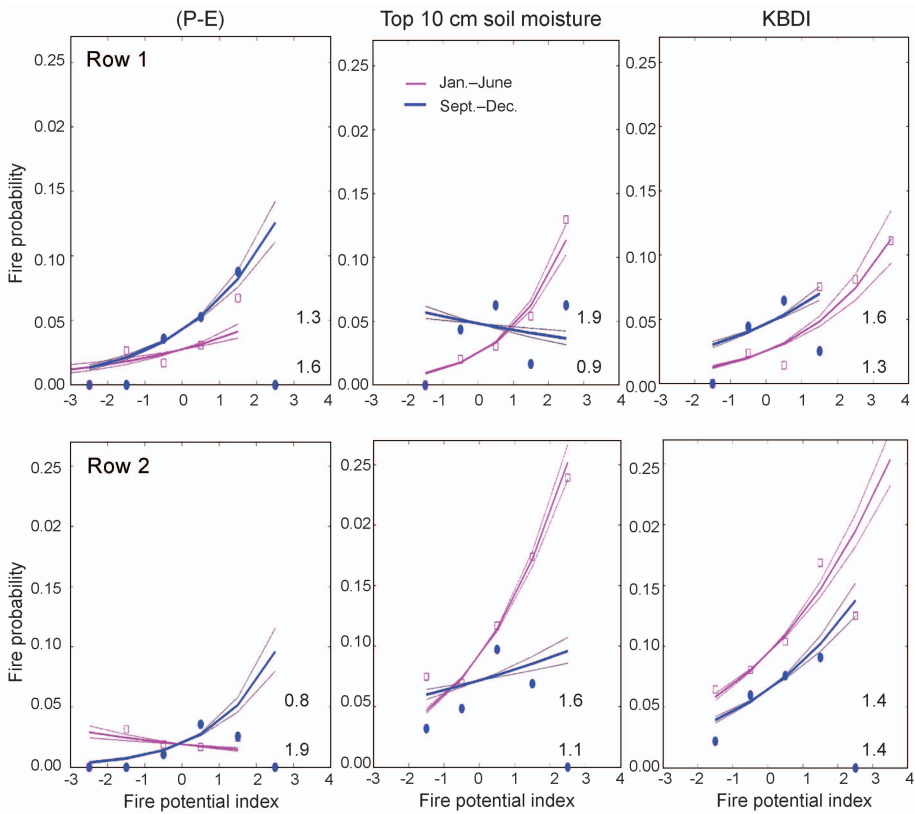


**Fig. 5.** Fire probability ( $p_i$ ) dependence on the fire potential index estimated from  $P-E$  (left column), the top 10 cm soil moisture (middle), and from  $KBDI$  (right column) data at selected grid cells shown in Figure 6. Row number (from 1 to 4) corresponds to the cell number shown in Figure 6. Solid lines represent fitted logistic model. Thin lines indicate uncertainty of the logistic model due to standard sampling error of  $\alpha_i$ -parameter estimate. Squares and filled circles correspond to January–mid-June and to mid-September–December period, respectively. The fire odds factor ( $\exp[\alpha_i]$ ) is shown by numbers in the lower right corner of each frame for January–mid-June (upper value) and for mid-September–December (lower). Figure continues on facing page.

The scale of the fire risk index ( $x_i$ ) was represented by unit intervals beginning at  $-2.5$  and ending at  $3.5$ , as illustrated in Figure 5. Before fitting into logistic model, the  $x_i$  values estimated from accumulated ( $P-E$ ) and the top 10 cm soil moisture data were multiplied by  $-1$ . This multiplication provides a common sign for the  $x_i$  scale (positive end of the  $x_i$  scale stands for increasing of wildfire probability) for all three indexes used in this study (i.e., increases in the index would lead to increases in wildfire likelihood). Due to a relatively small number of sample points around end intervals of  $x_i$ , empirical estimates of fire probability might be statistically unstable and this could affect estimates of logistic model parameters. Therefore weighting factors were applied within each  $i$  interval to represent the data uncertainty/variance. The weights

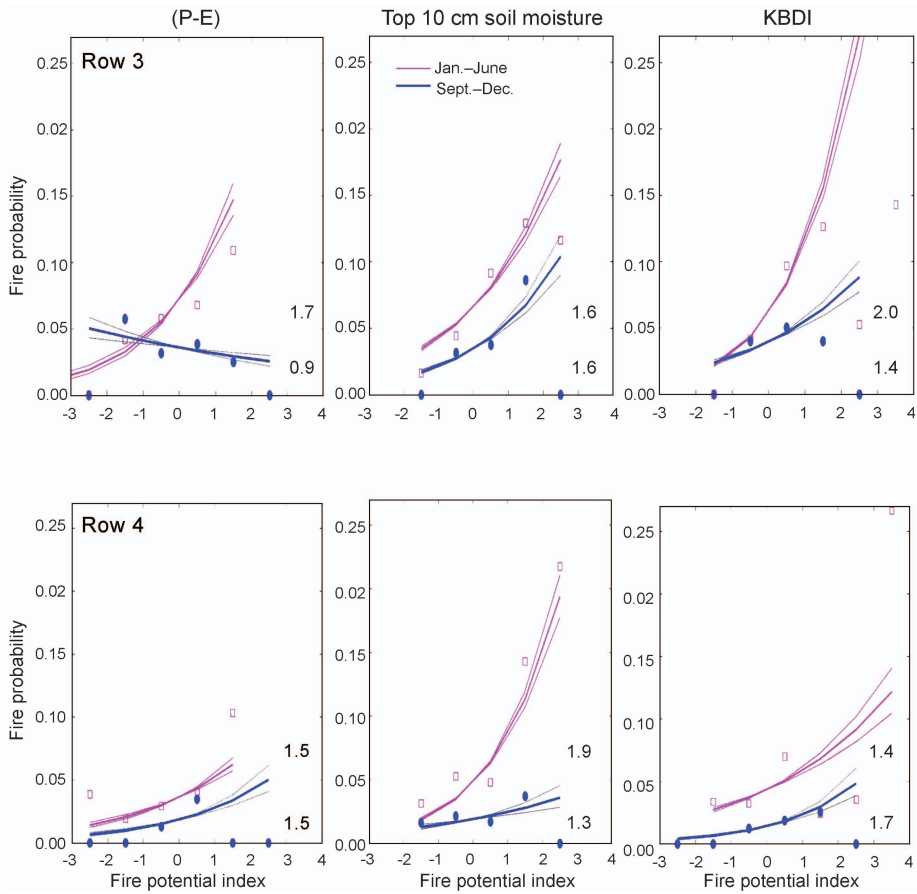
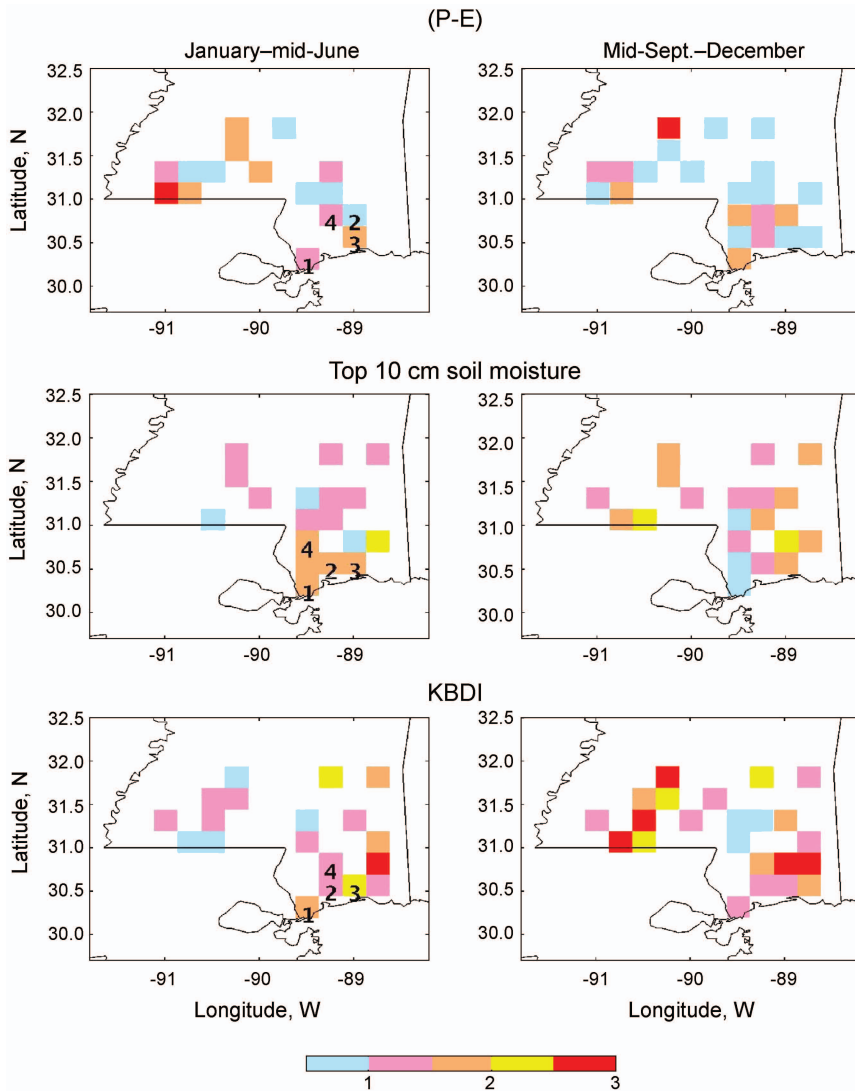


Fig. 5. continued.

were assumed to be proportional to the expected number of sample points within each  $i$  interval of  $x_i$ .

Figure 5 exemplifies the fitted dependence between fire probability ( $p_i$ ) and the fire potential index  $x_i$  based on accumulated ( $P-E$ ), the top 10 cm soil moisture, and  $KBDI$  at four grid cells selected within the Mississippi Gulf Coast zone. The locations of these cells are depicted by numbers (from 1 to 4) in Figure 6. There is an overall good agreement between logistic model  $p_i$  and empirical estimates of fire probability shown in Figure 5 by squares and filled circles corresponding to January–mid-June and to the mid-September–December period, respectively. The preliminary nature of this study (to illustrate and test a concept of using NLDAS-based fire potential indices) and a limited record of years (23) resulted in a small number (2–3) of sample points within end intervals of  $x_i$ , and thus the agreement between model-fitted and empirical estimates has not been quantified numerically. For that reason, use of a simple qualitative criterion of agreement based on squared residuals might be inappropriate. In most cases shown in Figure 5, the fire odds factor ( $F = \exp[\alpha_1]$ ) exceeds 1, implying that fire odds increase  $F$ -times in response to unit change in  $x_i$ . In all cases estimated  $\alpha_1$ -values



**Fig. 6.** Geographical distribution of fire odds factor ( $\exp[\alpha_1]$ ) associated with different fire potential risk indices. Based on *P-E* (upper row), derived from the top 10 soil moisture (middle), and *KBDI*-based (lower row). Numbers stand for rows in Figure 5.

were statistically significant with a corresponding probability of at least 0.01 (usually less than that) of obtaining a non-zero  $\alpha_1$  by random chance. Note that the larger factor  $F$ , the stronger will be the control/impact of soil moisture on fire odds or probability. A certain consistency of  $F$ -values and fitted  $p_i$ -fire potential index curves is observed among the different fire risk indexes. Generally, all three fire indexes show higher  $F$ -values for January–mid-June than for the mid-September–December period.

The fire potential indices based on the top 10 cm soil moisture and *KBDI* have the largest impact on the wildfire odds (increasing it by almost 2 times in response to

each unit change of the corresponding fire potential index during the January–mid-June period and by nearly 1.5 times during mid-September–December) observed over  $0.25^\circ \times 0.25^\circ$  cells located along the state of Mississippi coastline as illustrated in Figures 5 and 6. These results suggest a rather strong control of soil moisture–based fire potential indices (based on the top 10 cm soil moisture and *KBDI*) on fire occurrence probability over this region.

## CONCLUSIONS

Use of NLDAS-2 gridded atmospheric data for fire regional risk assessment and mapping was demonstrated. Note that previous similar studies used only station observations (point data). It was shown that fire potential indexes based on the top 10 cm soil moisture and *KBDI* have the largest impact on the wildfire odds (increasing it by almost 2 times in response to each unit change of the corresponding fire risk index during the January–mid-June period and by nearly 1.5 times during mid-September–December) observed over  $0.25^\circ \times 0.25^\circ$  cells located along the Mississippi Coast.

The regression model representing fire probability as a logistic function of the fire potential indices based on different soil moisture estimates could provide a useful decision support tool for forest managers. The logistic modeling framework is flexible, so the current time-space resolution can be easily refined to meet users' specific requirements, when sufficiently long occurrence fire records are available. The current space-time resolution ( $0.25^\circ$  latitude-longitude and five days) of the logistic model is mostly limited by fire data availability. Also, it is quite reasonable to expect that incorporation of additional independent variables/covariates, such as vegetation indexes (NDVI and others) and use of time-lagged variables that quantify antecedent conditions, might improve prediction capabilities of the current logistic model. It also could be promising to optimize the fire potential indices by merging soil moisture fields simulated by various land surface models available from NLDAS-2 (e.g., Mosaic, Noah, SAC, and VIC models).

## ACKNOWLEDGMENTS

This research was supported by the NASA Applied Sciences Program via grant/project NNX10AB74G. Valentine Anantharaj was also supported by the National Center for Computational Sciences at the Oak Ridge National Laboratory, USA. The authors greatly appreciate efforts of the NLDAS-2 team for providing high-quality land surface data for the research community, and the efforts of the Mississippi Forestry Commission for continuing to supply wildfire data for research purposes.

## REFERENCES

- Albini, F. A. and E. D. Reinhardt, 1995, "Modeling Ignition and Burning Rate of Large Woody Natural Fuels," *International Journal of Wildland Fire*, 5:81–91.
- Anderson, K., Martell, D. L., Flannigan, M. D., and D. Wang, 2000, "Modeling of Fire Occurrence in the Boreal Forest Region of Canada," in *Fire, Climate Change and Carbon Cycling in North American Boreal Forests*, Kasischke, E. (Ed.), New York, NY: John Wiley and Sons, 357–367.



- Bradstock, R. A., Cohn, J. S., Gill, A. M., Bedward, M., and C. Lucas, 2009, "Prediction of the Probability of Large Fires in the Sydney Region of South-Eastern Australia Using Fire Weather," *International Journal of Wildland Fire*, 18:932–943.
- Chéret, V. and J.-P. Denux, 2011, "Analysis of MODIS NDVI Time Series to Calculate Indicators of Mediterranean Fire Susceptibility," *GIScience & Remote Sensing*, 48:171–194.
- Chladil, M. A. and M. Nunez, 1995, "Assessing Grassland Moisture and Biomass in Tasmania—the Application of Remote Sensing and Empirical Models for a Cloudy Environment," *International Journal of Wildland Fire*, 5:165–171
- Choi, J., Cooke, W. H., and M. D., Stevens, 2009, "Development of a Water Budget Management System for Fire Potential Mapping," *GIScience & Remote Sensing*, 46:39–53.
- Chou, Y. H., Minnich, R. A., and R. A. Chase, 1993, "Mapping Probability of Fire Occurrence in San Jacinto Mountains, California, USA," *Environmental Management*, 17:129–140.
- Cooke, W. H., Grala, K., and C. L. Wax, 2008, "A Method for Estimating Pan Evaporation for Inland and Coastal Regions of Southeastern U.S.," *Southeastern Geographer*, 48:149–171.
- Cosgrove, B. A., Lohmann, D., Mitchell, K. E., Houser, P. R., Wood, E. F., Schaake, J. C., Robock, A., et al., 2003, "Real-Time and Retrospective Forcing in the North American Land Data Assimilation System," *Journal of Geophysical Research*, 108(D22):8842 [doi: 10.1029/2002JD003118].
- Dimitrakopoulos, A. P., Mitsopoulos, I. D., and K. Gatoulas, 2010, "Assessing Ignition Probability and Moisture of Extinction in a Mediterranean Grass Fuel," *International Journal of Wildland Fire*, 19:29–34.
- Finney, M.A., 2005, "The Challenge of Quantitative Risk Analysis for Wildland Fire," *Forest Ecology and Management*, 211:97–108.
- Grala, K. and W. H. Cooke, 2010, "Spatial and Temporal Characteristics of Wildfires in Mississippi, USA," *International Journal of Wildland Fire*, 19:14–28.
- Heim, R. R., Jr., 2002, "A Review of Twentieth Century Drought Indices Used in the United States," *Bulletin of the American Meteorological Society*, 83:1149–1165.
- Janis, M. J., Johnson, M. B., and G. Forthun, 2002, "Near-Real Time Mapping of Keetch-Byram Drought Index in the South-Eastern United States," *International Journal of Wildland Fire*, 11:281–289.
- Jazwinski, A. H., 1970, *Stochastic Processes and Filtering Theory*, New York, NY: Academic Press, 376 p.
- Keetch, J. J. and G. M. Byram, 1968, *A Drought Index for Forest Fire Control*, Asheville, NC: United States Department of Agriculture, Forest Service Research Paper SE-38, 32 p.
- Koster, R. and M. J. Suarez, 1992, "Modeling the Land Surface Boundary in Climate Models as a Composite of Independent Vegetation Stands," *Journal of Geophysical Research*, 97(D3):2697–2715.
- Kumar, S. V., Peters-Lidard, C. D., Eastman, J. L., and W.-K. Tao, 2008, "An Integrated High-Resolution Hydrometeorological Modeling Testbed Using LIS and WRF," *Environmental Modeling and Software*, 23:169–181.
- Luo, L., Robock, A., Mitchell, K. W., Houser, P. R., Wood, E. F., Schaake, J. C., Lohmann, D., et al., 2003, "Validation of the North American Land Data Assimilation System

- (NLDAS) Retrospective Forcing over the Southern Great Plains,” *Journal of Geophysical Research*, 108:8843 [doi:10.1029/2002JD003246].
- Manabe, S. and T. Delworth, 1990, “The Temporal Variability of Soil Wetness and its Impact on Climate,” *Climatic Change*, 16:185–192.
- McCullagh, P. and J. A. Nelder, 1991, *Generalized Linear Models*, 2nd ed., New York, NY: Chapman and Hall.
- Mesinger, F., DiMego, G., Kalnay, E., Mitchell, K., Shafran, P. C., Ebisuzaki, W., Jovic, D., et al., 2004, “North American Regional Reanalysis,” in *Proceedings of the 20th International Conference on Interactive Information and Processing Systems (IIPS) for Meteorology, Oceanography, and Hydrology*, Seattle, WA: 84th AMS Annual Meeting, 13 p. (CD-ROM).
- Mitchell, K. E., Lohmann, D., Houser, P. R., Wood, E. F., Schaake, J. C., Robock, A., Cosgrove, B. A., et al., 2004, “The Multi-institutional North American Land Data Assimilation System (NLDAS): Utilizing Multiple GCIP Products and Partners in a Continental Distributed Hydrological Modeling System,” *Journal of Geophysical Research*, 109:D07S90 [doi:10.1029/2003JD003823].
- NOAA NCDC (National Oceanic and Atmospheric Administration, National Climate Data Center), 2009, *Climate Data Online* [<http://cdo.ncdc.noaa.gov/CDO/cdo>].
- Pellizzaro, G., Cesaraccio, C., Duce, P., Ventura, A., and P. Zara, 2007, “Relationships between Seasonal Patterns of Live Fuel Moisture and Meteorological Drought Indices for Mediterranean Shrubland Species,” *International Journal of Wildland Fire*, 16:232–241.
- Pook, E. W. and A. M. Gill, 1993, “Variation of Live and Dead Fine Fuel Moisture in *Pinus radiata* Plantations of the Australian Capital Territory,” *International Journal of Wildland Fire*, 3:155–168.
- Preisler, H. K., Brillinger, D. R., Burgan, R. E., and J. W. Benoit, 2004, “Probability-Based Models for Estimation of Wildfire Risk,” *International Journal of Wildland Fire*, 13:133–142.
- Reardon, J., Hungerford, R., and K. Ryan, 2007, “Factors Affecting Sustained Smouldering in Organic Soils from Pocosin and Pond Pine Woodland Wetlands,” *International Journal of Wildland Fire*, 16:107–118.
- Swain, S., Wardlow, B. D., Narumalani, S., Tadesse, T., and K. Callahan, 2011, “Assessment of Vegetation Response to Drought in Nebraska Using Terra-MODIS Land Surface Temperature and Normalized Difference Vegetation Index,” *GIScience & Remote Sensing*, 48:432–455.
- Wilks, D. S., 2006, *Statistical Methods in the Atmospheric Sciences*, 2nd ed., New York, NY: Academic Press, 627 p.
- Zhai, Y. S., Munn, I. A., and D. L. Evans, 2003, “Modeling Forest Fire Probabilities in the South-Central United States Using FIA Data,” *Southern Journal of Applied Forestry*, 27:11–17.